

# Microstructure Characterization and Corrosion Properties of Nitrocarburized AISI 4140 Low Alloy Steel

M. Fattah and F. Mahboubi

(Submitted April 5, 2010; in revised form March 8, 2011)

Plasma nitrocarburizing treatments of AISI 4140 low alloy steel have been carried out in a gas mixture of 85% N<sub>2</sub>-12% H<sub>2</sub>-3% CO<sub>2</sub>. All treatments were performed for 5 h at a chamber pressure of 4 mbar. Different treatment temperatures varying from 520 to 620 °C have been used to investigate the effect of treatment temperature on the corrosion and hardness properties and also microstructure of the plasma nitrocarburized steel. Scanning electron and optical microscopy, x-ray diffraction, microhardness measurement, and potentiodynamic polarization technique in 3.5% NaCl solution were used to study the treated surfaces. The results revealed that plasma nitrocarburizing at temperatures below 570 °C can readily produce a monophasic  $\epsilon$  compound layer. The compound layer formed at 620 °C is composed of two sub-layers and is supported by an austenite zone followed by the diffusion layer. The thickest diffusion layer was related to the sample treated at 620 °C. Microhardness results showed a reduction of surface hardness with increasing the treatment temperature from 520 to 620 °C. It has also been found that with increasing treatment temperature from 520 to 545 °C the corrosion resistance increases up to a maximum and then decreases with further increasing treatment temperature from 545 to 620 °C.

**Keywords** AISI 4140 steel, austenitic plasma nitrocarburizing, corrosion resistance, electrochemical property, ferritic plasma nitrocarburizing, hardness

the corrosion resistance of the nitrocarburized AISI 4140 low alloy steel.

## 1. Introduction

Nitrocarburizing is a thermochemical process which involves the introduction of nitrogen and carbon atoms into the component surface. The microstructure of a nitrocarburized sample is generally composed of a thin compound layer and diffusion zone underneath (Ref 1). Plasma nitrocarburizing treatments can be classified into ferritic and austenitic treatment categories. Ferritic nitrocarburizing is mainly applied to steels to improve surface properties by a compound layer which consists mainly of  $\gamma'$  and  $\epsilon$  phases and is supported by a diffusion zone underneath (Ref 2, 3).  $\epsilon$  phase has better corrosion resistance than  $\gamma'$  phase (Ref 4). Ferritic and austenitic plasma nitrocarburizing processes have been attempted for the production of a monophasic  $\epsilon$  compound layer (Ref 5). Some data relating properties of plasma nitrocarburizing of AISI 4140 low alloy steel have been published in the past (Ref 6, 7). The objective of this work is to study the influence of ferritic and austenitic plasma nitrocarburizing treatment at different temperatures on the characteristic of the nitrocarburized layers, hardness, and corrosion resistance of AISI 4140 low alloy steel. The results are used to compare the effect of thickness, type, and the amount of carbonitride formed in the compound layer and the characteristic of the treated surface on

## 2. Material and Methods

AISI 4140 disk samples with the chemical composition of (in wt.%): 0.39% C; 0.93% Cr; 0.67% Mn; 0.2% Si; 0.15% Mo; and balance Fe, 20 mm in diameter and 8 mm thick, were placed on the substrate for plasma nitrocarburizing. Surface of the specimens was mechanically ground by 120-, 400-, 600-, 800-, and 1200-grit wet SiC emery paper and fine polished with alumina slurry to yield a mirror finish. The experiments were performed in a 5 kW pulsed cold wall plasma processing unit, using a gas composition of 85% N<sub>2</sub>-12% H<sub>2</sub>-3% CO<sub>2</sub> at 520, 545, 570 °C for ferritic and 620 °C for austenitic nitrocarburizing at a pressure of 4 mbar for 5 h in the range of 600-700 V discharge voltage and 2-3 A current. After finishing plasma treatment, the vacuum chamber was pumped down to 10<sup>-2</sup> Torr and then all samples were cooled to room temperature with the average rate of 5 °C/min. The treated specimens were sectioned for metallographic examination. In order to retain the edges during metallographic preparation, the cut segments were nickel electroplated in a Watts bath. The microstructure was revealed using 2% nital for ferrite-treated samples and a reagent composed of 1 cc conc. HCl mixed with 15 cc ethanol, 1 cc mix in addition to 99 cc of 2% nital (Ref 8) for austenite-treated samples. The cross section of the treated specimens was studied using optical and Philips XL30 scanning electron microscopy. The phases existing in the surface layers were identified using XRD analyzer with CuK $\alpha$  ( $\lambda = 1.5418 \text{ \AA}$ ) radiation. The variation in structural composition across the compound layers was determined by removal of different thicknesses from the surface using 1200 grade SiC

M. Fattah and F. Mahboubi, Department of Mining and Metallurgical Engineering, Amirkabir University of Technology, Hafez Ave, P.O. Box 15875, 4413 Tehran, Iran. Contact e-mail: mahboubi@aut.ac.ir.

abrasive. After each removal, the samples were analyzed with x-ray diffraction analyzer. Surface hardness and hardness profile were determined using a Shimadzu-type B Vickers microhardness tester with 25 and 50 g load for hardness profile and surface hardness, respectively. At least three measurements were taken to determine the exact value of each point. The electrochemical characterization was performed by potentiodynamic polarization test using an Autolab model PGSTAT20 in 3.5 wt.% NaCl solution with a scan rate of 1 mV/s. The tester was connected to a standard three-electrode cell comprising the sample as the working electrode, a saturated Calomel reference electrode, and a platinum counter electrode.

### 3. Results and Discussion

#### 3.1 Microstructure and XRD

SEM micrographs from the cross section of nitrocarburized specimens are shown in Fig. 1. The results revealed that the thickness of the compound layer is affected by the treatment temperature. Increase in compound layer thickness with increasing the treatment temperature from 520 to 620 °C is attributed to the greater amount of the interaction between iron atoms and highly reactive nitrogen and carbon atoms in the plasma near the surface as well as the higher diffusion of nitrogen and carbon atoms through the compound layer at higher treatment temperature (Ref 9, 10).

As it can be seen in the SEM micrographs (Fig. 1a to c), the microstructure of the samples nitrocarburized at temperatures below 570 °C is composed of a compound layer and diffusion zone. However, nitrocarburizing at 620 °C produced three different zones: a compound layer, a diffusion zone, and a thin and noncontinuous transformed austenite zone in between, Fig. 1(d). The compound layer in the specimen treated at

620 °C consists of two sub-layers: a porous layer at the top of the compound layer and a columnar pattern structure layer in the inner part of that. Upper porous layer, columnar structure part of the compound layer, and transformed austenite zone are clearly visible in the optical micrograph of sample nitrocarburized at 620 °C, Fig. 2. Dark area next to the compound layer is the transformed austenite zone. The outer part of the compound layer is continuous with some pores due to the accumulation and recombination of atomic nitrogen at the grain boundaries (Ref 11). In austenitic nitrocarburizing, the austenite region, which is formed near the compound layer, transforms to ferrite and Fe<sub>4</sub>N phases and causes a microstructure which is called braunite to produce during slow cooling of the sample to room temperature (Ref 12). Since the samples were slowly cooled in the chamber, the white area in Fig. 1(d) and the dark area in Fig. 2, between the compound layer and diffusion zone, is the transformed austenite region to braunite. Any visible peak of

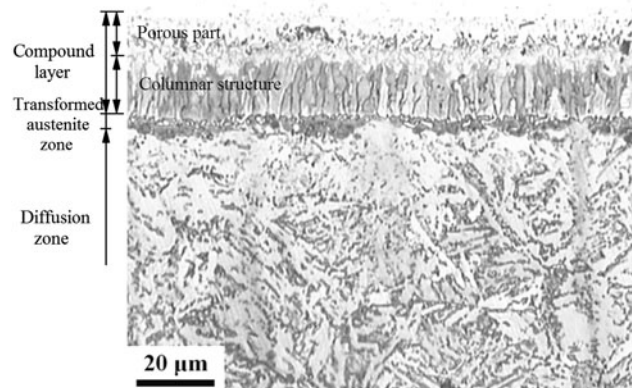


Fig. 2 Optical micrograph of cross section of plasma nitrocarburized AISI 4140 steel at 620 °C

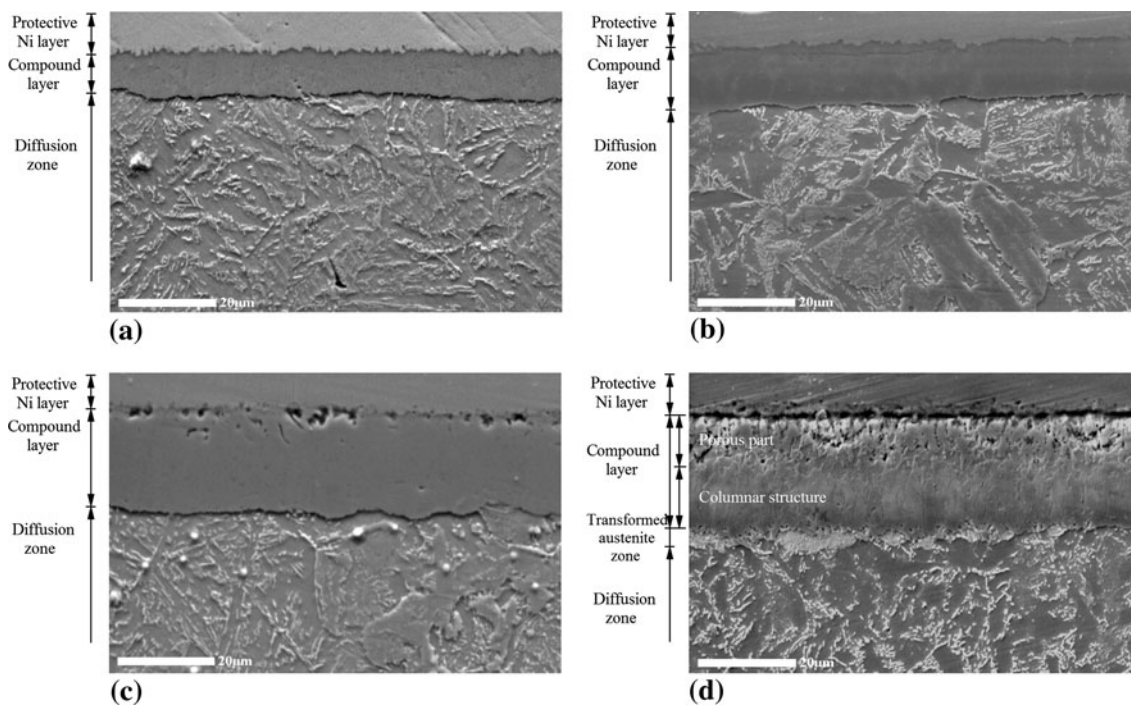
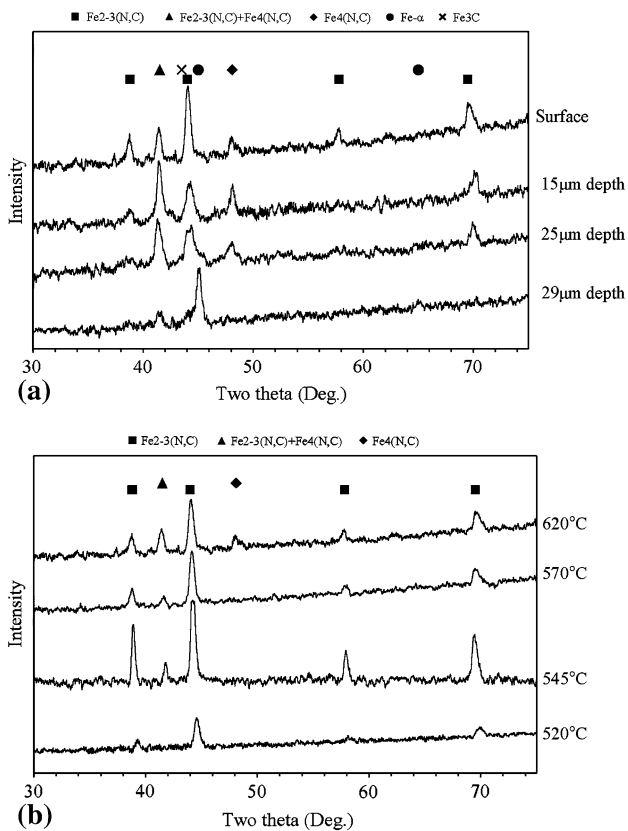


Fig. 1 SEM images of cross section of AISI 4140 steel plasma nitrocarburized at (a) 520 °C, (b) 545 °C, (c) 570 °C, and (d) 620 °C



**Fig. 3** XRD results of plasma nitrocarburized AISI 4140 steel from (a) different depths of the compound layer formed at 620 °C and (b) compound layer surface at different temperatures

austenite was not detected in Fig. 3(a) because austenite is transformed to braunite (Fe- $\alpha$  and Fe $_4$ N) phase during slow cooling and also no austenite was remained.

Figure 3(a) shows XRD patterns of different depths of the two sub-layer compound layer and transformed austenite zone formed at 620 °C. The results revealed that the upper porous sub-layer of the compound layer is mainly composed of  $\epsilon$  phase and the columnar pattern structure layer (bottom part of the compound layer in the depth of 15  $\mu$ m from the surface) is a mixed phase layer composed of  $\epsilon$  and  $\gamma'$ . From the results, it can be also seen that the amount of  $\epsilon$  phase decreased from the surface to the bottom of the compound layer and the amount of  $\gamma'$  phase increased. The columnar pattern structure and the reduction of  $\epsilon$  phase in the columnar pattern layer in comparison to the upper part of the compound layer is related to the formation of a low nitrogen content  $\epsilon$  phase during high temperature nitrocarburizing, which tends to decompose into  $\gamma'$  and  $\epsilon$  during slow cooling of sample (Ref 3). At the depth of 25  $\mu$ m from the surface the amount of carbonitride phases decreases and a small amount of Fe- $\alpha$  and Fe $_3$ C in the interface of the compound layer/austenite zone was detected. Fe $_3$ C formation is due to the enrichment of the bottom part of the compound layer with carbon in nitrocarburizing of low alloy steels (Ref 8).

The XRD patterns of the plasma nitrocarburized samples in Fig. 3(b) show that with increasing the treatment temperature from 520 to 545 °C, the intensity of  $\epsilon$  carbonitride phase in the surface increased. The increase of the  $\epsilon$  carbonitride intensity in the compound layer is related to the higher interaction between

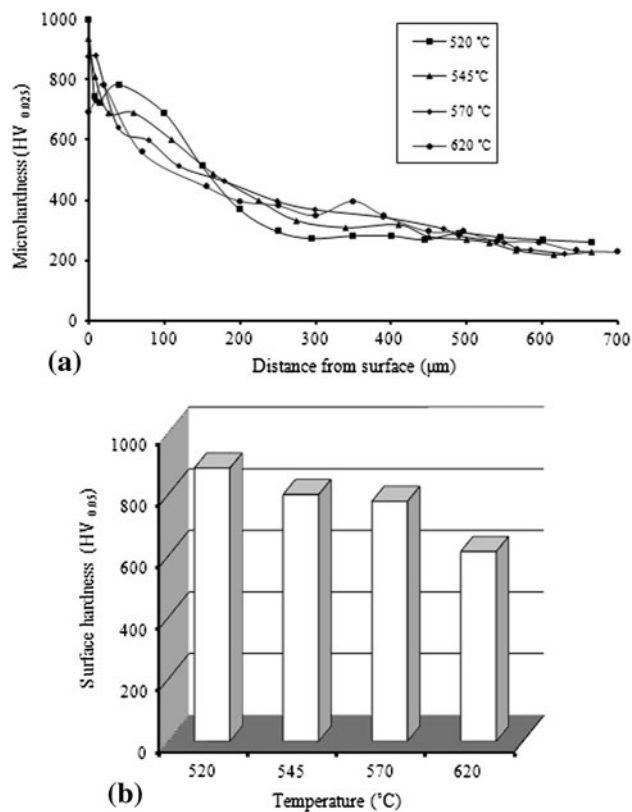


**Fig. 4** (a) Microhardness profiles and (b) surface hardness of AISI 4140 steel plasma nitrocarburized at different temperatures

detached iron atoms near the surface and also increased diffusion coefficient of nitrogen at the higher temperatures (Ref 9, 10). Decrease in the intensity of carbonitride peak in the compound layer with increasing in temperature to 570 °C is possibly attributed to the porous surface of the compound layer formed at 570 °C. After treatment temperature has increased from 570 to 620 °C,  $\gamma'$  carbonitride phase was produced along with  $\epsilon$  phase. As mentioned before, this can be attributed to the decomposition of low nitrogen content  $\epsilon$  phase formed at 620 °C into  $\gamma'$ ,  $\epsilon$ , and Fe- $\alpha$  during slow cooling of sample. Therefore, a more  $\epsilon$  dominance compound layer is formed during ferritic plasma nitrocarburizing (Fig. 3b). Since the compound layer is quite thick, the XRD results do not show the phase constitution of the whole compound layer due to the low penetration depth of Cu K $\alpha$  x-rays in steel.

### 3.2 Microhardness

Microhardness profiles (Fig. 4a) were used to determine the diffusion zone thickness. The case depth is defined as the depth at which the hardness is 10% above the core hardness. The results show that total case depth increases from 350 to 540  $\mu$ m with increasing the treatment temperature from 520 to 620 °C. The thickest case depth (540  $\mu$ m) is observed in the sample treated at 620 °C, in which the maximum hardness is reached in the middle part of the compound layer and a continuous decrease in hardness from the middle of the compound layer toward both the surface and the core of the specimen is observed. In contrast, the hardness profiles of the treated samples at 520, 545, and 570 °C have a continuous decrease from the surface toward the core of the specimen.

The surface hardness results are shown in Fig. 4(b). It is found that the surface hardness is decreased with increasing treatment temperature from 520 to 620 °C. The highest surface hardness (886 HV0.05) is achieved in sample nitrocarburized at 520 °C.

The depth of the nitrogen and carbon atoms diffusion can be affected by the treatment temperature. The case depth is governed by the diffusion of atoms through the material. Increasing the treatment temperature results in an increased atom diffusion coefficient and the carbon and nitrogen atoms penetrate in more distances from the surface (Ref 13). Therefore, with increasing the treatment temperature from 520 to 620 °C the case depth increased.

The reduction in hardness inside the compound layer toward the surface in the sample treated at 620 °C is regarded as the results of the porous zone that extends from the surface through the compound layer. Broaden and deep porous zone near the surface can be considered as the main reason for the hardness drop in the surface in the hardness profile.

At higher treatment temperature, coarser nitrides and carbonitrides with limited gain in hardness are formed. The hardness trend with increasing the treatment temperature also depends on the stability of the nitrides and carbonitrides at the higher temperatures (Ref 14). On the other hand, the amount of porosities affects the hardness in the compound layer. As it is shown in Fig. 1, deeper porous zone in the compound layer was formed at 570 and 620 °C with respect to those which were formed at 520 and 545 °C. Thus, the enlargement of carbonitrides, solution of carbonitrides and the formation of the deep porous zone in the compound layer with increasing the treatment temperature can be considered as the reasons for the hardness reduction after increasing the treatment temperature.

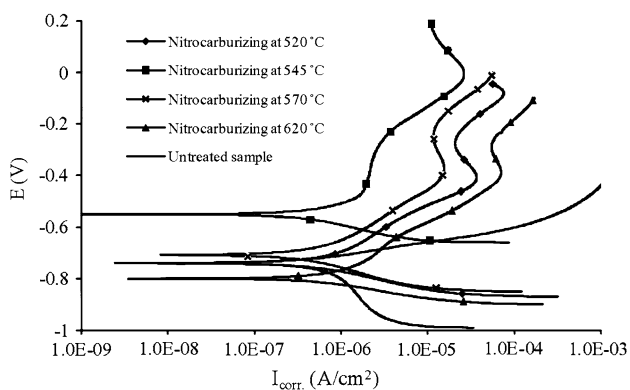


**Fig. 5** Potentiodynamic polarization curves for untreated and treated AISI 4140 low alloy steel at different temperatures

**Table 1** Polarization test results

Sample code	Plasma treatment	Temperature, °C	$E_{\text{corr.}}$ , V	$I_{\text{corr.}}$ , A/cm <sup>2</sup>	Corrosion rate, mm/year
1	Nitrocarburizing	520	-0.74	$1.57 \times 10^{-6}$	$3.64 \times 10^{-2}$
2		545	-0.56	$4.5 \times 10^{-7}$	$1.06 \times 10^{-2}$
3		570	-0.70	$1.4 \times 10^{-6}$	$3.22 \times 10^{-2}$
4		620	-0.8	$1.86 \times 10^{-6}$	$4.31 \times 10^{-2}$
5	Untreated sample	...	-0.74	$1.95 \times 10^{-6}$	$4.537 \times 10^{-2}$

### 3.3 Electrochemical Properties

Figure 5 and Table 1 present the results of potentiodynamic polarization test of samples nitrocarburized at different temperatures as well as the untreated sample. The results show that with an increase of treatment temperature from 520 to 545 °C, corrosion potential increases, whereas corrosion current density decreases. However, with the more increase of treatment temperature to 570 and 620 °C, corrosion potential reduces and corrosion current density rises. Nevertheless, the lowest corrosion current density was observed in the sample treated at 545 °C. Figure 6 shows the optical micrograph from cross section of the sample treated at 620 °C after the polarization test. From the micrograph, it can be seen that there are some corrosion pits in the upper part of the compound layer which provide a direct path for the corrosive medium penetration through the compound layer to the columnar pattern structure inner layer. More detail information was given in our previous article (Ref 15).

The potential difference of a phase or material, which is used as a coating with respect to the substrate, defines the ability of the coating to protect the substrate material against electrochemical corrosion. Carbonitrides such as  $\gamma'$  ( $\text{Fe}_4\text{N}_3\text{C}$ ) and  $\epsilon$  ( $\text{Fe}_{2-3}\text{N}_3\text{C}$ ) are noble phases and are positive with respect to steel in electrochemical series (Ref 16, 17). Hence, they provide mechanical protection while they remain intact (Ref 16). Therefore, after plasma nitrocarburizing, the corrosion resistance increases due to the formation of iron carbonitride phases on the surface.

As iron nitrides are noble phases, the denser the nitrides, the better the protective quality (Ref 17). Thus, increase in  $E_{\text{corr}}$  with increasing in nitrocarburizing temperature from 520 to 545 °C is attributed to the thicker compound layer and higher amount of carbonitride formed at 545 °C with respect to 520 °C, as shown in Fig. 1(a), (b) and 3(b).

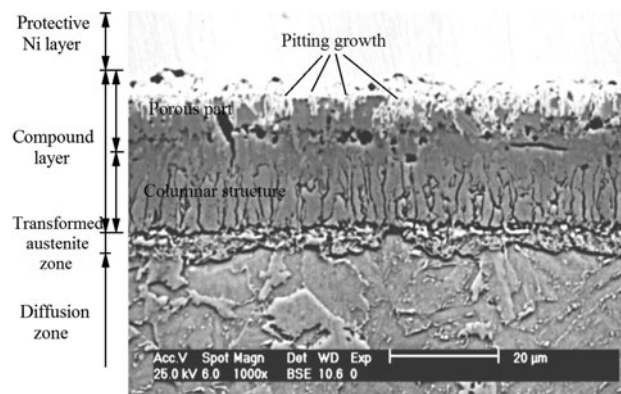


**Fig. 6** SEM image of cross section of AISI 4140 steel plasma nitrocarburized at 620 °C after the polarization test

Defects on the surface such as pores affect the corrosion resistance of the surface. The oxygen concentration at the valleys and the tops of the pores is different during the polarization test. Therefore, the valleys and the tops act as local anode and cathode, respectively, leading to the formation of pits (Ref 18). So the pitting corrosion behavior is due to the porous compound layer. From Fig. 1, it can be seen that the amount of pores increased with increasing the treatment temperature from 545 to 570 and 620 °C and the most porous compound layer was related to the sample treated at 620 °C. Figure 6 shows that the pitting growth begins from pores in the upper layer of the compound layer. The amount of pits in the sample treated at 620 °C with the higher amount of pores in the compound layer is more than that of treated sample at 570 °C. Cross-sectional micrograph for sample treated at 570 °C after polarization test and detail information were reported previously (Ref 15).

In the other hand,  $\epsilon$  phase has better corrosion resistance with respect to the  $\gamma'$  phase owing to its crystalline structure and higher nitrogen content (Ref 5). Therefore, the corrosion resistance improvement of the surface after nitrocarburizing depends on the type of the phases formed in the compound layer. The amount of  $\epsilon$  phase in the compound layer is the most important parameter for improving the general and localized corrosion resistance of the treated surface. Furthermore, the corrosion resistance of the surface increases with increasing the amount of  $\epsilon$  phase in the compound layer (Ref 19). It can be observed from Fig. 3(b) that with the increase in treatment temperature from 570 to 620 °C the intensity of  $\epsilon$  phase decreased and  $\gamma'$  phase was formed in the compound layer. Thus, decrease in corrosion resistance with increasing the treatment temperature from 545 to 570 and 620 °C is probably due to the pitting corrosion in the porous compound layer formed at 570 and 620 °C as well as the reduction of  $\epsilon$  and formation of  $\gamma'$  in the compound layer.

#### 4. Conclusions

This research demonstrates that the possibility of  $\gamma'$  phase formation and thickness of the compound layer and diffusion zone increases by increasing the treatment temperature from 520 to 620 °C. In austenitic plasma nitrocarburizing at 620 °C, a thin austenite zone was formed beneath the compound layer and the type and the amount of the carbonitride phases varied from the surface to the bottom part of the compound layer. The compound layer formed on the treated sample at 545 °C showed the maximum amount of  $\epsilon$  phase. In the austenitic-treated sample at 620 °C, the maximum hardness across the compound layers was seen in the middle part of the compound layer which decreased with a sharp reduction in the outer part of the compound layer. Nitrocarburizing can improve the corrosion resistance of the surface. Corrosion resistance improvement is affected by the amount and type of the carbonitride phases formed in the compound layer and the

compound layer thickness and also the amount of surface porosity. The effect of type of the carbonitride phase in the compound layer and the characteristic of the compound layer surface is more dominant than the effect of compound layer thickness on the corrosion resistance.

#### References

1. T. Malinava, S. Malinov, and N. Pantev, Simulation of Microhardness Profiles for Nitrocarburized Surface Layers by Artificial Neural Network, *Surf. Coat. Technol.*, 2001, **135**(2–3), p 258–267
2. A. Suhadi, C.X. Li, and T. Bell, Austenitic Plasma Nitrocarburising of Carbon Steel in N<sub>2</sub>-H<sub>2</sub> Atmosphere with Organic Vapour Additions, *Surf. Coat. Technol.*, 2006, **200**, p 4397–4405
3. T. Bell, Y. Sun, and A. Suhadi, Environmental and Technical Aspects of Plasma Nitrocarburizing, *Vacuum*, 2000, **59**, p 14–23
4. D. Oliveira, A.P. Tschiptschin, and C.E. Pinedo, Simultaneous Plasma Nitriding and Ageing Treatments of Precipitation Hardenable Plastic Mould Steel, *Mater. Des.*, 2007, **28**, p 1714–1718
5. T. Bell, M. Kinali, and G. Munstermann, Physical Metallurgy Aspects of the Austenitic Nitrocarburising Process, *Heat Treat. Met.*, 1987, **2**, p 47–51
6. M. Karakan, A. Alsaran, and A. Celik, Effect of Process Time on Structural and Tribological Properties of Ferritic Plasma Nitrocarburized AISI, 4140 Steel, *Mater. Des.*, 2004, **25**, p 349–353
7. I. Lee, Plasma Post Oxidation of Nitrocarburized AISI, 4140 Steel, *Rare Met.*, 2006, **25**, p 267–271
8. E. Haruman, T. Bell, and Y. Sun, The Compound Layer Characteristics Resulting from Plasma Nitrocarburizing with an Atmosphere Containing CO<sub>2</sub> Gas Additions, *Surf. Eng.*, 1993, **3**, p 121–140
9. B. Edenhofer, Physical and Metallurgical Aspects of Ion Nitriding, *Heat Treat. Met.*, 1974, **1**, p 59–67
10. F. Mahboubi and K. Abdolvahabi, The Effect of Temperature of Plasma Nitriding Behavior of DIN 1.6959 Low Alloy Steel, *Vacuum*, 2006, **81**, p 239–243
11. S. Li, R.R. Manory, and J.H. Hensler, Compound Layer Growth and Compound Layer Porosity of Austenite Plasma Nitrocarburized Non-Alloyed Steel, *Surf. Coat. Technol.*, 1995, **71**, p 112–120
12. G.E. Totten and A.H. Hawes Maurice, *Steel Heat Treatment Handbook*, 2nd ed., Taylor and Francis Group, New York, 2007
13. D.A. Porter and K.E. Easterling, *Phase Transformation in Metals and Alloys*, VNB, UK, 1983
14. R.S.E. Schneider and H. Hiebler, Influence of Increased Nitriding Temperatures on the Hardness Profile of Low-Alloy Steels, *J. Mater. Sci.*, 1998, **33**, p 1737–1744
15. M. Fattah and F. Mahboubi, Comparison of Ferritic and Austenitic Plasma Nitriding and Nitrocarburizing Behavior of AISI, 4140 Low Alloy Steel, *Mater. Des.*, 2010, **31**, p 3915–3921
16. C. Dawes, D.F. Tranter, and C.G. Smith, Reappraisal of Nitrocarburizing and Nitriding When Applied to Design and Manufacture of Non-Alloy Steel Automobile Components, *J. Heat Treat.*, 1979, **1**(2), p 30–42
17. A. Basu, J. Dutta Majumdar, J. Alphonsa, S. Mukherjee, and I. Manna, Corrosion Resistance Improvement of High Carbon Low Alloy Steel by Plasma Nitriding, *Mater. Lett.*, 2008, **62**, p 3117–3120
18. R. Winston Revie and H.H. Uhlig, *Corrosion and Corrosion Control*, 4th ed., Wiley, Hoboken, NJ, 2008
19. D.C. Wen, Microstructure and Corrosion Resistance of the Layers Formed on the Surface of Precipitation Hardenable Plastic Mold Steel by Plasma-Nitriding, *Appl. Surf. Sci.*, 2009, **256**, p 797–804